Published in final edited form as:
Bone. 2007 December ; 41(6): 995–1004. doi:10.1016/j.bone.2007.08.020.

Transgenic Over-expression of Plasminogen Activator Inhibitor-1 Results in Age-dependent and Gender-specific Increases in Bone Strength and Mineralization

S.M. Nordstrom[1], **S.M. Carleton**[2], **W.L. Carson**[3], **M. Eren**[1], **C.L. Phillips**[2], and **D.E. Vaughan**[1]

[1]Departments of Medicine and Pharmacology, Vanderbilt University, Nashville Tennessee

[2]Department of Biochemistry, University of Missouri- Columbia, Columbia Missouri

[3]Comparative Orthopaedic Laboratory, University of Missouri-Columbia, Columbia, Missouri

Abstract

The plasminogen activation system (PAS) and its principal inhibitor, plasminogen activator inhibitor- 1 (PAI-1), are recognized modulators of matrix. In addition, the PAS has previously been implicated in the regulation of bone homeostasis. Our objective was to study the influence of active PAI-1 on geometric, biomechanical, and mineral characteristics of bone using transgenic mice that over-expresses a variant of human PAI-1 that exhibits enhanced functional stability.

Femora were isolated from male and female, wildtype (WT) and transgenic (PAI-1.stab) mice at 16 and 32 weeks of age (n=10). Femora were imaged via DEXA for BMD and μCT for cortical mid-slice geometry. Torsional testing was employed for biomechanical properties. Mineral composition was analyzed via instrumental neutron activation analysis. Female femora were further analyzed for trabecular bone histomorphometry (n=11). Whole animal DEXA scans were performed on PAI-1.stab females and additional transgenic lines in which the functional domains of the PAI-1 protein were specifically disrupted.

Thirty-two week female PAI-1.stab femora exhibited decreased mid-slice diameters and reduced polar moment of area compared to WT, while maintaining similar cortical bone width. Greater biomechanical strength and stiffness was demonstrated by 32 week PAI-1.stab female femora in addition to a 52% increase in BMD. PAI-1.stab trabecular bone architecture was comparable to WT. Osteoid area was decreased in PAI-1.stab mice while mineral apposition rate increased by 78% over WT. Transgenic mice expressing a reactive-site mutant form of PAI-1 showed an increase in BMD similar to PAI-1.stab, whereas transgenic mice expressing a PAI-1 with reduced affinity for vitronectin were comparable to WT.

Over-expression of PAI-1 resulted in increased mineralization and biomechanical properties of mouse femora in an age-dependent and gender-specific manner. Changes in mineral preceded increases in strength/stiffness and deterred normal cross-sectional expansion of cortical bone in females. Trabecular bone was not altered in PAI-1.stab mice whereas MAR increased significantly, further supporting mineral changes as the underlying factor in strength differences. The primary influence of PAI-1 occurred during a period of basal bone remodeling, attributing a

Correspondence to: Douglas E. Vaughan, M.D., Division of Cardiovascular Medicine, Vanderbilt University Medical Center, 383 PRB, 2220 Pierce Ave, Nashville, TN 37232, Phone: 615-936-1719, Fax: 615-936-2936, Douglas.E.Vaughan@vanderbilt.edu.

role for this system in remodeling as opposed to development. Comparison of transgenic lines indicates that PAI-1's influence on bone is dependent on its ability to bind vitronectin, and not on its proteolytic activity. The impact of PAI-1 on mouse femora supports a regulatory role of the plasminogen activation system in bone homeostasis, potentially elucidating novel targets for the treatment of bone disease.

INTRODUCTION

The quality and composition of bone extracellular matrix (ECM) is a principal factor determining bone strength, as matrix serves as both a scaffold for mineralization and an active signaling module to bone cells through protein expression. [15, 48] Bone matrix is produced and mineralized by osteoblast cells and maintained by the coordinate actions of osteoblasts, osteoclasts, and osteocytes. The complex composition of bone ECM is dependent on a variety of factors, involving the precise assembly of collagen fibrils and the repertoire of non-collagenous proteins which include the regulated expression and activity of adhesion molecules. [9, 64] These constituents affect cell migration, cell adhesion, and the activity of osteoblasts and osteoclasts. Systems that regulate ECM production and remodeling are potential therapeutic targets for the reduction of fracture risk.

The plasminogen activation system (PAS) is a well-characterized regulator of matrix remodeling, primarily identified for its role in the fibrinolytic system. Its principal inhibitor, plasminogen activator inhibitor-1 (PAI-1), has been of particular focus in cardiovascular disease due to the strong positive correlation between serum PAI-1 levels and cardiovascular risk. Specifically, elevated serum PAI-1 is recognized as an independent determinant of risk for myocardial infarction (MI). [56] Increased circulating PAI-1 is also correlated with incidence of recurrent MI, angina pectoris, and atherosclerosis. [29–31, 53] In addition to cardiovascular disease, PAI-1 and the PAS play an integral role in cancer progression; PAI-1 is one of the most informative prognostic markers in several cancers. [1, 19] PAI-1 is also reported to be involved in pathological processes such as asthma, insulin resistance, and obesity. [37] PAI-1 production is stimulated by various factors, including glucose, insulin, angiotensin II, and fatty acids. [41, 43, 60] In addition, a common polymorphism exists in the promoter region of the PAI-1 gene that plays an important role in determining plasma PAI-1 levels. [24] Together, these factors indicate the commonality of elevated circulating PAI-1 and the clinical significance of the PAS and its primary inhibitor across multiple systems.

The PAS culminates in the conversion of the inactive proenzyme, plasminogen, to the active serine protease, plasmin. This proteolytic event is mediated by tissue-type (t-PA) and urokinase (uPA) plasminogen activators and is inhibited through the action of PAI-1. [59] PAI-1 is a 47kDa single-chain glycoprotein member of the serine protease inhibitor (SERPIN) family, and is functionally and structurally unstable. The active conformation spontaneously converts to latency with a rapid half-life; however, active PAI-1 can be stabilized through binding to substrates such as vitronectin (VN). Active PAI-1 covalently interacts with t-PA and uPA resulting in rapid inactivation of the plasminogen activators and clearance of complexes via an LDL receptor-related protein 1 (LRP1)-dependent mechanism. [17] Through its interaction with t-PA and uPA, PAI-1 can blunt plasminogen activation and matrix degradation. PAI-1 also indirectly decreases ECM degradation by reducing plasmin-mediated activation of matrix metalloproteinases (MMPs). [62] Independent of its proteolytic function, PAI-1 can alter matrix through high affinity binding to vitronectin, competing with integrin interactions and thereby modulating cell adhesion and cell migration. Recently, Vial *et al*. reported that PAI-1 can enhance the activation of β1 integrin and assembly of fibronectin through a uPAR ligand- and vitronectin-dependent

mechanism. [61] Others have described the influence of PAI-1 on additional matrix components, including transforming growth factor-beta (TGF-β), matrix γ-carboxyglutamic acid (Gla) protein, and osteocalcin. [20, 40, 42, 51] Additionally, PAI-1 and the plasminogen activators are expressed by bone cells and their substrate, plasminogen, is present in bone matrix. [34, 57] Taken together, it is clear that PAI-1 is topologically and functionally poised to influence bone matrix biology, and we therefore hypothesize that PAI-1 is a significant regulator of bone remodeling.

A limited number of studies have previously addressed this question and provide evidence in support of this hypothesis. Study of t-PA/uPA double knockout (t-PA$^{-/-}$/uPA$^{-/-}$) mice showed that lack of plasminogen activators resulted in increased trabecular bone volume (BV/TV) in the proximal tibia in newborn mice. This was associated with alterations in the composition of long bone, including increased mineral (calcium and phosphorous) and proteinaceous content (osteocalcin, fibronectin, and proteoglycan). [12] Osteoblasts isolated from t-PA$^{-/-}$/uPA$^{-/-}$ mice exhibit enhanced proliferation, differentiation, type I collagen secretion, and mineral deposition. [12] Co-cultures of t-PA$^{-/-}$/uPA$^{-/-}$ osteoblasts and osteoclasts demonstrated a reduction in non-mineralized matrix resorption. [13] In contrast, studies of PAI-1 knockout mice (PAI-1$^{-/-}$) from 8–17 weeks of age do not identify any clear bone phenotype and have apparently normal BV/TV, cortical thickness, and cortical bone mineral density compared to wild-type (WT) mice. However, significant differences were observed in the setting of estrogen-deficiency; PAI-1 deficiency appears to confer protection against ovariectomy-induced trabecular bone loss. [14] In humans, PAI-1 deficiency is extremely rare, while PAI-1 excess is an increasingly common condition, given its association with visceral obesity, insulin resistance, and the post-menopausal state in women. [27, 32, 38, 54] In this study, we aimed to characterize the bone phenotype of mice that over-express a variant of human PAI-1 where four mutations (N150H, K154T, Q319L and M354I) have been introduced to stabilize the protein in its active conformation. We hypothesized that increased PAI-1 activity would alter the biomechanical macroscopic properties of femoral cortical bone and its microscopic material properties through an alteration of bone morphology and/or mineralization.

MATERIALS AND METHODS

Animals

Studies were performed on femora from mice that over-express a stable variant of human PAI-1, referred to as PAI-1.stab. [23] This variant contains four mutations (N150H, K154T, Q319L, M354I) that function to stabilize the protein in its active conformation and it is expressed under the control of the preproendothelin-1 promoter. [4] Prior to this study, PAI-1.stab mice on a B6D2 mixed background were backcrossed seven times to C57BL/6J mice (Jackson Labs, Bar Harbor ME) to produce a homogenous background. Wild-type (WT) C57BL/6J mice (Jackson Labs, Bar Harbor ME) were housed with PAI-1.stab mice for a period ≥ 2 months. An independent comparison of femora from Jackson Labs mice with WT PAI-1.stab littermates showed no significant difference in bone mineral density *(data not shown)*.

Male and female mice were sacrificed via cervical dislocation at predefined time points corresponding with peak femoral bone mineral density and length (16 weeks) and during a period of basal bone remodeling (28 and 32 weeks)(n≥10). [3,25] Right and left hindlimbs were isolated, cleaned of surrounding tissue, and stored in phosphate buffered saline soaked gauze at −80°C for cortical bone analysis and strength determination. For trabecular bone analysis, isolated hindlimbs were immediately fixed in 10% neutral buffered formalin for 24 hours, cleaned of surrounding tissue, and placed in fresh fixative.

Additional transgenic lines on the B6D2 background, referred to as Q123K PAI-1.stab and R346A PAI-1.stab *(described recently* [22]), were analyzed for total skeletal bone mineral density during basal bone remodeling (39–43 weeks). Q123K PAI-1.stab mice over-express stable human PAI-1 with an additional mutation in the vitronectin (VN)-binding site of the protein which reduces the affinity of PAI-1 for VN while maintaining SERPIN activity. [36] R346A PAI-1.stab mice over-express stable human PAI-1 with an additional mutation in the reactive-center loop that eliminates SERPIN activity while maintaining normal VN binding. [55] Measures of Q123K PAI-1.stab mice and R346A PAI-1.stab mice were normalized to WT age-matched littermates. All animals were given access to standard rodent diet, water, and activity *ad libitum*.

Cortical Bone Geometry

Geometric data was collected from left femora by μCT scan analysis [MicroCATII® (Imtek, Bridgeport NJ): exposure time = 300msecs, voltage = 80kVp, current = 500μA]. Amira3.1® software (Mercury Computer Systems, Chelmsford MA) was used to create a 3-dimensional reconstruction of the μCT image slices, determine total femur length, and to identify the femoral mid-slice. The mid-slice was modeled as a hollow ellipse with periosteal ($_p$) and endosteal ($_e$) anterior-posterior minor diameters (d_p, d_e) and medio-lateral major diameters (D_p, D_e). [10] Amira3.1® analysis software allows pixels to be plotted across the major and minor axes, forming a histogram that represents pixel density (P) across the mid-slice. The bone density threshold of $[P_{max} + (P_{max}\text{-}P_{min})/3]$ was empirically set based on histologic measures and was consistently applied in determination of bone cortical edges from WT and PAI-1.stab femora. Cortical bone width is reported as the average of four measurements on the major and minor axes. The polar moment of area type parameter (K) was calculated using: $K=[(\pi D_p^3 d_p^3)(1\text{-}q^4)]/[16(D_p^2+d_p^2)]$, where $q= D_e/D_p$. [50]

Trabecular Bone Histology and Histomorphometry

Mice were injected intra-peritoneally with tetracycline hydrochloride (Sigma, St. Louis MO) at 25 mg/kg twelve days and two days prior to sacrifice. Undemineralized femora were embedded in methyl methacrylate and longitudinal sections (5 μm, 10 μm) were cut using a Leica 2265 microtome (Vashaw Scientific, Norcross GA). Five μm sections were stained with Goldner's Trichrome stain for static measurements. Ten μm sections were left unstained for dynamic measurements. A region of interest was selected 1mm distal to the growth plate extending 2 mm downward through the metaphysis of the femur, avoiding the primary spongiosa. Standard bone histomorphometry was performed by the methods of Parfitt *et al* using Bioquant image analysis software (R & M Biometrics, Nashville, TN). [44] Four types of primary measurements were made: area, length/perimeter, distance between points or lines, and number. Referents, such as tissue volume, bone volume, bone surface, and osteoid surface were used to derive other indices, such as trabecular number and trabecular separation. Fluorescent measurements were made of interlabel width wherefrom mineral apposition rate was calculated by applying the interlabel period.

Biomechanical Testing

To assess the macroscopic strength and stiffness of the femoral diaphysis and its corresponding microscopic cortical bone material properties, we subjected the isolated femora to testing by torsional load to failure. For each femur, a steel cylindrical holder was machined with two diametrically opposite side windows and two struts that aligned the ends of the cylinder and protected the bone until testing. The diaphyseal axis of the femur was centered using paper washers on each end of the window, creating an exposed test section of length L. The epiphyseal ends of the femur were secured with epoxy. A custommade tweezer device was used to hold the cylinder ends in line while the struts were severed using

a cut off wheel (Dremel, Racine WI). The cylinder was then placed in a pure torsional load test fixture mounted on a TA-HDi testing machine (Stable Micro Systems, Surrey UK). A cross bar prevented rotation of the femur's proximal end, while the distal end was rotated about the long axis at a constant speed of 0.75 radians/sec. The test machine's control software recorded its crosshead position and cable force (F) at a rate of 200 samples/sec. A digital camera was used to take pre- and post-test photos of each specimen, as well as a video-audio clip of each test to obtain a record of the mode of femur failure. Applied torque (T) was calculated using $T=[(F - F_{\text{friction in fixture}})*0.13006]$. T was then plotted as a function of relative angular displacement (θ) between the ends of the exposed section of femur shaft. Femoral diaphysis ultimate torsional strength (T_{max}) was taken as the absolute peak torque and torsional stiffness (K_s) as the slope of a line fit by linear regression between 5–10 Nmm applied torque or in an overlapping-adjacent region if a localized anomaly occurred. Strain energy to failure (U) was calculated as the area under the 'applied torque vs angular displacement' curve up to T_{max}. The microscopic cortical bone material properties, ultimate tensile strength (Su) and shear modulus of elasticity (G), were calculated using $Su=16T_{max} / [\pi D_p (d_p^2) (1-q^4)]$ and $G=K_sL / K$, where L=7mm. [50]

Mineral Composition

Isolated left femora were analyzed for bone mineral density (BMD) by dual-energy x-ray absorptiometry (DEXA) using a Hologic QDR-1000W scanner in conjunction with Hologic high-resolution software version 4.76 for adaptation to small animal imaging (Hologic, Bedford MA). Total skeletal BMD (whole animal) was determined by DEXA using a PIXImus II mouse densitometer in conjunction with manufacturer supplied software (GE Lunar, Madison WI). Densitometer stability was controlled by phantom scanning prior to each set of measurements. Mice were anesthetized with pentobarbital intra-peritoneally at 50 mg/kg. The skull region was excluded in determination of density. Additionally, instrumental neutron activation analysis (NAA) was employed to quantify individual elements that comprise the mineralized matrix. Isolated right femora were demarrowed, defatted, and lyophilized, then irradiated to create a radioactive nuclide. Based on signature gamma ray emissions, levels of fluorine (F), magnesium (Mg), sodium (Na), chloride (Cl), calcium (Ca), phosphorous (P), potassium (K), and zinc (Zn) were quantified in each femur and normalized to the mass of the bone sample as previously described. [46]

Plasma PAI-1 Levels

Plasma was collected from mice by retro-orbital bleeding at a fixed time of day between 12pm and 1pm. Circulating PAI-1 antigen levels were determined in duplicate using a TintElize PAI-1 EIA kit against human PAI-1 antigen (Trinity Biotech, St Louis MO).

Statistical Analysis

Data analyses were performed in GraphPad Prism version 4.00® for Windows statistical software (GraphPad Software, San Diego CA). Results are expressed as mean ± standard deviation. Where three or more groups are compared, significance was determined by one-way ANOVA followed by Tukey's multiple comparison post-test. Mean difference and 95% confidence interval of the mean difference is reported for select groups. A two-tailed t-test was applied where only two groups are compared. Normalization of transgenic whole animal BMD measurements to age-matched, background-matched WT controls was achieved with the baseline-correction function, indicating unmatched replicates. For each set of normalized ratios, a one-sample t-test with a theoretical mean = 1 was used to determine significance from WT. $\alpha=0.05$ was set for all statistical analyses.

RESULTS

Cortical Bone Geometry

Analysis of the femoral mid-shaft slice revealed significant geometric differences between WT and PAI-1.stab mice. Femora from 32 week old PAI-1.stab females exhibited significantly decreased periosteal/endosteal diameters across the major and minor axes of the cortical bone. In contrast, these parameters did not differ between PAI-1.stab and WT females at 16 weeks of age (Fig. I, Table I). Femora from 32 week old PAI-1.stab males demonstrated decreased periosteal/endosteal diameters across the major axis and 16 week PAI-1.stab males had reduced periosteal diameters across the major axis compared to age- and gender-matched WT. Furthermore, WT females demonstrated significant age-dependent increases in periosteal/endosteal diameters across the major and minor axes of the cortical bone from 16 to 32 weeks of age. Similar age-dependent changes were not reflected in PAI-1.stab females, nor in males of either genotype. Cortical bone width did not differ as a function of age or genotype. Cortical bone area was reduced for all PAI-1.stab groups, only reaching significance in 32 week PAI-1.stab males. The polar moment of area type parameter (K) was significantly reduced in 32 week PAI-1.stab females. Total femur length was comparable between genotypes in all gender and age groups (Table I).

Trabecular Bone Histology and Histomorphometry

Analysis of trabecular bone from female mice at an age corresponding with basal bone remodeling revealed no significant genotypic differences in measures of trabecular architecture, including bone volume, trabecular thickness, and trabecular spacing. In contrast, osteoid surface was decreased by 90% in PAI-1.stab femora compared to WT and mineral apposition rate was concomitantly increased by 78% (Table II, Fig. II).

Biomechanical Properties

Biomechanical testing revealed increased femoral diaphysis ultimate torsional strength in 32 week PAI-1.stab females compared to age-matched WT females. This group also trended toward increased torsional stiffness, although statistical significance was not achieved (mean difference= −8.57: 95% CI= −20.35 to 3.20). Femora from 16 week females, 16 week males, and 32 week males showed no differences in strength or stiffness with respect to genotype (Figs. IIIA & C, Table III). Strain energy to failure was not statistically different between genotypes in all groups. Combining torsional testing data with geometric parameters of the femoral mid-slice, we determined biomechanical parameters of the bone material, independent of femur dimensions. Femora from WT females exhibited an age-dependent reduction in cortical bone tensile strength (Su) and shear modulus of elasticity (G) from 16 weeks to 32 weeks of age. WT males demonstrated a decrease in bone tensile strength with age; however, shear modulus of elasticity remained unchanged. In contrast, PA1.stab females and males did not display this age-dependent reduction in bone material properties. Correspondingly, 32 week PAI-1.stab females exhibited significantly increased cortical bone tensile strength and shear modulus of elasticity compared to 32 week WT females (Figs. IIIB & D, Table III).

Mineral Composition

In agreement with their increased macroscopic (T_{max}) and microscopic (Su) strength parameters, isolated femora from 32 week PAI-1.stab females displayed greater BMD compared to age-matched WT females. No statistical difference was present in 16 week PAI-1.stab females, although a trend towards increased BMD was observed (mean difference= −0.015: 95% CI= −0.037 to 0.008). Femora isolated from 16 and 32 week

PAI-1.stab males showed no difference in BMD compared to age-matched WT mice (Fig. IV).

All PAI-1.stab groups had substantially reduced levels of F incorporation into the mineralized matrix, with the greatest reduction present in 32 week female femora compared to WT controls (64%). Mg and K levels differed significantly in 16 week PAI-1.stab females compared to WT. There was no impact of genotype on matrix incorporation of Ca, P, Na, or Zn, nor was the Ca/P ratio significantly altered (Table IV).

In agreement with femoral BMD, total skeletal BMD of PAI-1.stab females was significantly increased during basal bone remodeling compared to WT. Analysis of additional transgenic lines, Q123K PAI-1.stab and R346A PAI-1.stab, also revealed significant changes from WT littermates as well as from PAI-1.stab mice. Q123K PAI-1.stab mice have significantly reduced BMD compared to PAI-1.stab. Furthermore, Q123K PAI-1.stab mice have reduced BMD compared to WT littermates (Fig. V). Similar to PAI-1.stab, R346A PAI-1.stab mice display significantly increased total skeletal BMD compared to matched WT. This increase in BMD is also statistically greater than PAI-1.stab (Fig. V).

Circulating PAI-1 Levels

Plasma PAI-1 levels were comparable between all PAI-1.stab groups. Male PAI-1.stab mice exhibited circulating human PAI-1 antigen levels of 7.1 ± 1.2 ng/ml and 6.0 ± 1.7 ng/ml at 16 and 32 weeks, respectively. Female PAI-1.stab mice exhibited circulating levels of 5.4 ± 1.6 ng/ml and 4.4 ± 1.3 ng/ml at 16 and 32 weeks, respectively.

DISCUSSION

In a largely age-dependent and gender-specific manner, PAI-1 over-expression is associated with increased proximity of cortical bone to the central axis compared to WT, as reflected in decreased periosteal/endosteal mid-section major and minor diameters and reduced polar moment of area. With comparable cortical bone widths, these structural parameters are indicative of reduced femoral strength. [21] Importantly, WT female mice exhibited an age-dependent increase in all of the aforementioned parameters (Table I), a phenomenon supported by Brodt et al. which describes a significant increase in minor periosteal diameter, M-L moment of inertia, A-P moment of inertia, and polar moment of inertia in female C57Bl/6J femora from 16 to 24 weeks of age. [7] In contrast, PAI-1.stab females do not exhibit similar structural changes indicating that PAI-1 over-expression interferes with this age-related geometric alteration. Based on geometric parameters alone we would therefore expect that PAI-1.stab femora would demonstrate reduced torsional strength when compared to WT. This prediction proved to be incorrect however, as mechanical testing demonstrated an age-dependent and female gender-specific increase in diaphyseal ultimate torsional strength and stiffness of PAI-1.stab femora, apparently due to increased bone biomechanical properties. Analyses of the diaphyseal cortical bone strength and stiffness data combined with the mid-slice geometric parameters using classical mechanic’s equations permitted determination of the bone material properties, which are independent of femoral geometry. This analysis revealed greater bone material strength [bone tensile strength (Su)] and stiffness [shear modulus of elasticity (G)] in 32 week PAI-1.stab female femora compared to age-matched WT females. Thus, the greater torsional strength and stiffness of 32 week female PAI-1.stab femora can be attributed to increased bone material properties, which more than compensate for the reduced cross-sectional dimensions.

To further investigate the critical determinants of material composition, we analyzed the areal BMD of isolated femora and quantified individual elements that comprise the

mineralized matrix. The increased BMD of PAI-1.stab femora from 32 week females is in agreement with their increased macroscopic and microscopic strength, which is also consistent with the possibility that the observed increase in torsional strength can be attributed to altered material properties. Notably, 16 week females also exhibited a trend towards increased BMD. Analysis of the mineral composition indicated that all PAI-1.stab groups incorporated substantially less F into the mineralized matrix than WT controls, with the greatest reduction present in 32 week females (64%). F is reported to have a biphasic effect on bone strength. During bone formation, F incorporates into hydroxyapatite crystals by substituting for hydroxyl groups, creating a more thermodynamically stable and less soluble crystal. [28] At low levels of incorporation, this compacting effect increases the overall strength of bone. However, at high levels, bone becomes brittle and strength is compromised, which occurs in the murine model of *osteogenesis imperfecta* (*oim/oim*). [46,58] Optimal levels of F incorporation into the mineralized matrix are not quantitatively defined but, based on the reduced levels of F in PAI-1.stab femora and their tendency towards greater tensile strength, we suggest that this lower level of F incorporation creates a more ideal material with regard to strength properties. It is also interesting to note that, from 16 to 32 weeks of age, both WT and PAI-1.stab mice exhibited a significant increase in F content indicating that this basal remodeling period may be an important stage for F incorporation into bone. An additional mineral alteration was a reduction in Mg levels found in 16 week PAI-1.stab female femora. Mg has been reported to inhibit hydroxyapatite formation through competition with Ca at active growth sites. [2, 5] Low Mg incorporation increases the hydroxyapatite crystal size, whereas high Mg content has a compacting effect. [6, 8] Mg levels are elevated in *oim/oim* mice and in iliac crest biopsies from post-menopausal osteoporotic human females. [8, 46] Sixteen week PAI-1.stab females also demonstrated altered K levels. Despite changes in these trace minerals, Ca, P, and the Ca/P ratio were comparable between genotypes in all groups.

Considering the changes in F, Mg, and K levels, and the trend towards increased BMD in female PAI-1.stab mice at 16 weeks of age, it seems likely that changes in mineral composition of PAI-1.stab femora precede the measured geometric alterations. Increasing the distribution of bone from the central torsional axis, as demonstrated by the WT female mice from 16 to 32 weeks of age, is a normal mechanism by which bone structurally compensates for suboptimal mineral composition in the aging skeleton. [21] We hypothesize that PAI-1.stab mice derive a material strength benefit from these alterations in mineral composition that removes the stimulus to undergo compensatory structural remodeling, thereby explaining the contrasting finding of increased strength in geometrically weaker femora.

In support of the conclusions drawn from study of cortical bone, analysis of trabecular bone revealed no significant changes in trabecular bone architecture between PAI-1.stab and WT females. However, a significant decrease in the osteoid area of PAI-1.stab femora indicates either an increase in osteoblast- mediated resorption of non-mineralized matrix or increased mineralization of the osteiod to bone. The significant increase in mineral apposition rate in PAI-1.stab mice supports the latter; PAI-1.stab femora have reduced osteoid as a result of increased mineralization of the non-mineralized matrix to form bone. Based on dynamic and static measures of trabecular bone, we conclude that changes in PAI-1.stab females that result in increased femoral strength can be attributed to the mineral component of bone and are not architecturally based.

Analysis of the Q123K PAI-1.stab and R346A PAI-1.stab females provided additional insights into the mechanism by which PAI-1 influences mineralization. Study of these transgenic lines allow for separation of the two major functions of PAI-1, its proteolytic activity and matrix-binding ability, and assessment of the contribution of each *in vivo*. The

significant increase in BMD measured in R346A PAI-1.stab mice indicates that the bone phenotype of PAI-1.stab females is not dependent on the ability of PAI-1 to interact with plasminogen activators. In contrast, Q123K PAI-1.stab mice exhibited reduced BMD, thereby attributing the increased mineral and strength properties of PAI-1.stab femora to the VN-binding ability of the PAI-1 protein and distinguishing this phenotype from other recently described phenotypic alterations of PAI-1.stab mice dependent on proteolytic activity. [22] Differences in clearance of the R346A PAI-1.stab protein compared to PAI-1.stab may explain the greater BMD of R346A PAI-1.stab mice compared to PAI-1.stab. Whereas both proteins have similar affinities for mouse VN (*unpublished)*, after complexing with plasminogen activators (PA), PAI-1.stab loses its affinity for VN and the PAI-1-PA complexes are rapidly cleared through an LRP-dependent mechanism. [55] In contrast, the R346A PAI-1.stab protein is unable to form a covalent complex with plasminogen activators and therefore is not displaced from matrix VN. This may provide a partial explanation for the exaggerated bone phenotype seen in R346A PAI-1.stab mice. The mechanism behind the decreased BMD of Q123K PAI-1.stab mice compared to WT is less clear. Considering the opposite bone phenotypes achieved by separating the primary functions of the PAI-1 protein and the PAI-1.stab phenotype lying between these two extremes, two opposing mechanisms of PAI-1 in the regulation of bone homeostasis might exist. The matrix-binding function of PAI-1 may play a role in support bone mineralization while the proteolytic interaction with t-PA/uPA that ultimately impacts plamin generation and uPAR signaling may function to oppose mineralization. It is important to note that significant differences in body weight exist that may confound the analysis. Whereas PAI-1.stab mice have comparable body weight to WT, R346A PAI-1.stab mice have significantly greater body weight than matched WT and PAI-1.stab. In contrast, Q123K PAI-1.stab mice have significantly reduced body weights than matched WT and PAI-1.stab. Further studies are needed to explore these possibilities and further define the mechanism(s) by which PAI-1 influences bone homeostasis.

The present findings describing the influence of PAI-1 over-expression on bone homeostasis are largely consistent with previous reports, although biomechanical testing as performed here has not been described and previous cortical bone analyses are limited. Femora of female PAI-$1^{-/-}$ mice ages 8–17 weeks have been reported to be similar in length, calcium content, and cortical thickness compared to WT controls. [14] In addition, femoral BMD of PAI-$1^{-/-}$ mice did not differ from WT at 12 weeks, which agrees with our data at 16 weeks of age and supports the notion that the effect of the PAS on bone mineralization and strength is age-dependent. [14] Similarly, PAI-$1^{-/-}$ mice apparently show no phenotypic differences at 8–17 weeks in the properties of trabecular bone architecture, in agreement with our findings. [14] In contrast, t-$PA^{-/-}$ $uPA^{-/-}$mice reportedly exhibit increased femoral length, calcium content, trabecular bone volume and osteoid area at 5–7 days of age. [12] Although we cannot rule out a bone phenotype in 5–7 day old PAI-1.stab mice, our data indicates that any differences that may occur at this early stage in bone development return to normal by the time skeletal maturity is reached. Primary osteoblasts derived from t-$PA^{-/-}$ $uPA^{-/-}$ exhibit increased proliferation, differentiation, and mineral deposition. [12] Additional studies of PAI-1.stab primary cells are needed for comparison with published *in vitro* data and to further elucidate the mechanism that underlies this bone phenotype. Additionally, study of PAI-1.stab bone in the setting of estrogen-deficiency may reveal a differential response of bone to excess PAI-1 activity in the condition of accelerated bone turnover.

The present study is limited in several important aspects. The microscopic parameters of bone are calculated applying classical mechanics equations utilizing the femoral mid-slice geometric measurements. These calculations assume the bone cross-sectional geometry is uniform throughout the mouse femur, which does not accurately reflect the true structure of bone. Furthermore, the increased ultimate torsional strength, bone tensile strength, and shear

modulus of elasticity measured in 32 week female femora compared to age-matched WT females occurred in the absence of a significant change in strain energy to failure, which represents vulnerability to fracture during dynamic loading. Due to the variability of this parameter, larger sample sizes are needed to discern whether the significant macroscopic and microscopic strength parameters measured represent an increase in resistance to fracture during dynamic loading. An additional consideration lies in the transcriptional regulation of PAI-1.stab which in these transgenics is under the control of the preproendothelin-1 promoter. Whereas the native PAI-1 promoter directs expression of PAI-1 protein in osteoblast, osteoclast, osteocyte, smooth muscle, and endothelial cells, endothelin-1 is expressed in osteoblast, osteocyte, smooth muscle and endothelial cells, but not in osteoclasts. [33, 39, 63] PAI-1.stab therefore overlaps expression with native PAI-1 in most cells that influence bone, but is only poised to influence osteoclasts in a paracrine fashion. Despite the overlapping expression of these promoters, PAI-1's rapid secretion and primarily extracellular activity, and the close proximity of osteoblast and osteoclast cells, we cannot unequivocally state that excluding expression of PAI-1.stab in osteoclasts does not influence the phenotype.

The present study indicates that PAI-1 over-expression has a regulatory role in bone homeostasis through influence on the mineral composition of bone. Given that collagen serves as the structural template for mineral deposition, an underlying alteration in collagen chain structure, fibril cross-linkage, or alignment could lead to differences in mineral deposition in the osteoid. [9, 35] Considering the influence of PAI-1 on ECM components, further studies are needed to define the composition and quality of the organic matrix, especially collagen and the population of non-collagenous proteins (NCP). NCP profile differences between PAI-1.stab and WT mice may provide informative insights given that these proteins are thought to play important regulatory roles in mineralization. [64] Fibronectin, transforming growth factor-beta (TGF-β), matrix γ-carboxyglutamic acid (Gla) protein, and osteocalcin are not only integral components of the bone matrix, but the expression and/or activity of each of these NCPs is influenced by PAI-1. [20, 40, 42, 51] BMD measures of the Q123K PAI-1.stab and R346A PAI-1.stab indicated the importance of the high affinity binding of PAI-1 to vitronectin. Though this interaction, PAI-1 can influence integrin-, uPA receptor- (uPAR-), and fibronectin-dependent cellular interactions with the ECM and thereby alter cellular migration to and from sites of bone remodeling and cellular adhesion to the ECM and other cells. [11, 61] These non-proteolytic consequences of PAI-1 over-expression may disrupt interactions necessary for regulated osteoblast differentiation, osteoblast/osteoclast coupling, and bone cell response to environmental stimuli. [16, 52]

Others have proposed that interleukins impact the plasminogen activation system in bone. [14] Interleukin-6 knockout mice (IL-$6^{-/-}$) display a bone phenotype reminiscent of that seen in PAI-$1^{-/-}$ mice during both basal remodeling and in the setting of estrogen deficiency. [26, 47] In addition, double transgenic mice that co-express human IL-6 and the soluble IL-6 receptor phenotypically resemble some characteristics of PAI-1.stab mice, including hepatosplenomegaly as well as extramedullary hematopoesis. [45] Potentially, the phenotypic similarities between IL-6 double transgenic mice and PAI-1.stab mice as well as those between IL-$6^{-/-}$ mice and PAI-$1^{-/-}$ mice may reflect IL-6 regulation of *PAI-1*. [18] Alternatively, PAI-1 may influence the expression of *IL-6* or the two proteins may act through a common signaling pathway in the regulation of bone biology. [49]

Long-term increased expression of human PAI-1 influences bone homeostasis. The present findings provide additional evidence supporting an important role of the plasminogen activation system in the regulation of bone remodeling. The significance of PAI-1 in the determination of bone strength and fracture risk suggests that further investigations of this

matrix modulator and the PAS in relation to bone remodeling may help elucidate novel targets for pharmacologic treatment of bone disease.

Acknowledgments

We would like to acknowledge Carolyn Buff, PhD and J. Steve Morris, PhD at the University of Missouri-Columbia Research Reactor Center, as well as Timothy Hoffman, PhD, Chris Winkelmann, DVM, PhD, and Said Figueroa, PhD at the Biomolecular Imaging Center, Harry S. Truman Memorial Veterans Hospital, Columbia, MO, for their contributions to this project. We would also like to acknowledge the University of Alabama at Birmingham Center for Metabolic Bone Disease-Histomorphometry and Molecular Analysis Core Laboratory, supported by NIH Grant P30-AR46031, for trabecular bone analyses.

Funding Sources:

ROI HL51387, 2 T32 GM07628

REFERENCES

1. Andreasen PA, Egelund R, Petersen HH. The plasminogen activation system in tumor growth, invasion, and metastasis. Cell Mol Life Sci. 2000; 57:25–40. [PubMed: 10949579]
2. Aoba T, Moreno EC, Shimoda S. Competitive adsorption of magnesium and calcium ions onto synthetic and biological apatites. Calcif Tissue Int. 1992; 51:143–150. [PubMed: 1422954]
3. Beamer WG, Donahue LR, Rosen CJ, Baylink DJ. Genetic variability in adult bone density among inbred strains of mice. Bone. 1996; 18:397–403. [PubMed: 8739896]
4. Berkenpas MB, Lawrence DA, Ginsburg D. Molecular evolution of plasminogen activator inhibitor-1 functional stability. Embo J. 1995; 14:2969–2977. [PubMed: 7621813]
5. Bigi A, Foresti E, Gregorini R, Ripamonti A, Roveri N, Shah JS. The role of magnesium on the structure of biological apatites. Calcif Tissue Int. 1992; 50:439–444. [PubMed: 1596779]
6. Boskey AL, Rimnac CM, Bansal M, Federman M, Lian J, Boyan BD. Effect of short-term hypomagnesemia on the chemical and mechanical properties of rat bone. J Orthop Res. 1992; 10:774–783. [PubMed: 1403290]
7. Brodt MD, Ellis CB, Silva MJ. Growing C57Bl/6 mice increase whole bone mechanical properties by increasing geometric and material properties. J Bone Miner Res. 1999; 14:2159–2166. [PubMed: 10620076]
8. Burnell JM, Liu C, Miller AG, Teubner E. Effects of dietary alteration of bicarbonate and magnesium on rat bone. Am J Physiol. 1986; 250:F302–F307. [PubMed: 3946606]
9. Burr DB. The contribution of the organic matrix to bone's material properties. Bone. 2002; 31:8–11. [PubMed: 12110405]
10. Camacho NP, Hou L, Toledano TR, Ilg WA, Brayton CF, Raggio CL, Root L, Boskey AL. The material basis for reduced mechanical properties in oim mice bones. J Bone Miner Res. 1999; 14:264–272. [PubMed: 9933481]
11. Czekay RP, Aertgeerts K, Curriden SA, Loskutoff DJ. Plasminogen activator inhibitor-1 detaches cells from extracellular matrices by inactivating integrins. J Cell Biol. 2003; 160:781–791. [PubMed: 12615913]
12. Daci E, Everts V, Torrekens S, Van Herck E, Tigchelaar-Gutterr W, Bouillon R, Carmeliet G. Increased bone formation in mice lacking plasminogen activators. J Bone Miner Res. 2003; 18:1167–1176. [PubMed: 12854826]
13. Daci E, Udagawa N, Martin TJ, Bouillon R, Carmeliet G. The role of the plasminogen system in bone resorption in vitro. J Bone Miner Res. 1999; 14:946–952. [PubMed: 10352103]
14. Daci E, Verstuyf A, Moermans K, Bouillon R, Carmeliet G. Mice lacking the plasminogen activator inhibitor 1 are protected from trabecular bone loss induced by estrogen deficiency. J Bone Miner Res. 2000; 15:1510–1516. [PubMed: 10934649]
15. Dallas SL, Chen Q, Sivakumar P. Dynamics of assembly and reorganization of extracellular matrix proteins. Curr Top Dev Biol. 2006; 75:1–24. [PubMed: 16984808]

16. Damsky CH. Extracellular matrix-integrin interactions in osteoblast function and tissue remodeling. Bone. 1999; 25:95–96. [PubMed: 10423030]

17. DeClerck YA. Purification and characterization of a collagenase inhibitor produced by bovine vascular smooth muscle cells. Arch Biochem Biophys. 1988; 265:28–37. [PubMed: 2843102]

18. Dong J, Fujii S, Li H, Nakabayashi H, Sakai M, Nishi S, Goto D, Furumoto T, Imagawa S, Zaman TA, Kitabatake A. Interleukin-6 and mevastatin regulate plasminogen activator inhibitor-1 through CCAAT/enhancer-binding protein-delta. Arterioscler Thromb Vasc Biol. 2005; 25:1078–1084. [PubMed: 15718495]

19. Durand MK, Bodker JS, Christensen A, Dupont DM, Hansen M, Jensen JK, Kjelgaard S, Mathiasen L, Pedersen KE, Skeldal S, Wind T, Andreasen PA. Plasminogen activator inhibitor-I and tumour growth, invasion, and metastasis. Thromb Haemost. 2004; 91:438–449. [PubMed: 14983218]

20. Eeckhout Y, Vaes G. Further studies on the activation of procollagenase, the latent precursor of bone collagenase Effects of lysosomal cathepsin B, plasmin and kallikrein, and spontaneous activation. Biochem J. 1977; 166:21–31. [PubMed: 197917]

21. Einhorn TA. Bone strength: the bottom line. Calcif Tissue Int. 1992; 51:333–339. [PubMed: 1458335]

22. Eren M, Gleaves LA, Atkinson JB, King LE, Declerck PJ, Vaughan DE. Reactive site-dependent phenotypic alterations in PAI-1 transgenic mice. J Thromb Haemost. 2007

23. Eren M, Painter CA, Atkinson JB, Declerck PJ, Vaughan DE. Age-dependent spontaneous coronary arterial thrombosis in transgenic mice that express a stable form of human plasminogen activator inhibitor-1. Circulation. 2002; 106:491–496. [PubMed: 12135951]

24. Eriksson P, Kallin B, van't Hooft FM, Bavenholm P, Hamsten A. Allele-specific increase in basal transcription of the plasminogen-activator inhibitor 1 gene is associated with myocardial infarction. Proc Natl Acad Sci U S A. 1995; 92:851–855.

25. Ferguson VL, Ayers RA, Bateman TA, Simske SJ. Bone development and age-related bone loss in male C57BL/6J mice. Bone. 2003; 33:387–398. [PubMed: 13678781]

26. Franchimont N, Wertz S, Malaise M. Interleukin-6: An osteotropic factor influencing bone formation? Bone. 2005; 37:601–606. [PubMed: 16112634]

27. Gebara OC, Mittleman MA, Sutherland P, Lipinska I, Matheney T, Xu P, Welty FK, Wilson PW, Levy D, Muller JE, et al. Association between increased estrogen status and increased fibrinolytic potential in the Framingham Offspring Study. Circulation. 1995; 91:1952–1958. [PubMed: 7895352]

28. Grynpas MD. Fluoride effects on bone crystals. J Bone Miner Res. 1990; 5(Suppl 1):S169–S175. [PubMed: 2187325]

29. Hamsten A, de Faire U, Walldius G, Dahlen G, Szamosi A, Landou C, Blomback M, Wiman B. Plasminogen activator inhibitor in plasma: risk factor for recurrent myocardial infarction. Lancet. 1987; 2:3–9. [PubMed: 2885513]

30. Hamsten A, Wiman B, de Faire U, Blomback M. Increased plasma levels of a rapid inhibitor of tissue plasminogen activator in young survivors of myocardial infarction. N Engl J Med. 1985; 313:1557–1563. [PubMed: 3934538]

31. Juhan-Vague I, Alessi MC, Joly P, Thirion X, Vague P, Declerck PJ, Serradimigni A, Collen D. Plasma plasminogen activator inhibitor-1 in angina pectoris. Influence of plasma insulin and acute-phase response. Arteriosclerosis. 1989; 9:362–367. [PubMed: 2470343]

32. Juhan-Vague I, Alessi MC, Vague P. Increased plasma plasminogen activator inhibitor 1 levels A possible link between insulin resistance and atherothrombosis. Diabetologia. 1991; 34:457–462. [PubMed: 1916049]

33. Kitten AM, Andrews CJ. Endothelin-1 expression in long-term cultures of fetal rat calvarial osteoblasts: regulation by BMP-7. J Cell Physiol. 2001; 187:218–225. [PubMed: 11268001]

34. Knudsen BS, Silverstein RL, Leung LL, Harpel PC, Nachman RL. Binding of plasminogen to extracellular matrix. J Biol Chem. 1986; 261:10765–10771. [PubMed: 3090040]

35. Landis WJ. The strength of a calcified tissue depends in part on the molecular structure and organization of its constituent mineral crystals in their organic matrix. Bone. 1995; 16:533–544. [PubMed: 7654469]

36. Lawrence DA, Berkenpas MB, Palaniappan S, Ginsburg D. Localization of vitronectin binding domain in plasminogen activator inhibitor-1. J Biol Chem. 1994; 269:15223–15228. [PubMed: 7515053]
37. Lijnen HR. Pleiotropic functions of plasminogen activator inhibitor-1. J Thromb Haemost. 2005; 3:35–45. [PubMed: 15634264]
38. Lindeman JH, Pijl H, Toet K, Eilers PH, van Ramshorst B, Buijs MM, van Bockel JH, Kooistra T. Human visceral adipose tissue and the plasminogen activator inhibitor type 1. Int J Obes (Lond). 2007
39. Martin TJ, Allan EH, Fukumoto S. The plasminogen activator and inhibitor system in bone remodelling. Growth Regul. 1993; 3:209–214. [PubMed: 8130729]
40. Munger JS, Harpel JG, Gleizes PE, Mazzieri R, Nunes I, Rifkin DB. Latent transforming growth factor-beta: structural features and mechanisms of activation. Kidney Int. 1997; 51:1376–1382. [PubMed: 9150447]
41. Nilsson L, Banfi C, Diczfalusy U, Tremoli E, Hamsten A, Eriksson P. Unsaturated fatty acids increase plasminogen activator inhibitor-1 expression in endothelial cells. Arterioscler Thromb Vasc Biol. 1998; 18:1679–1685. [PubMed: 9812904]
42. Novak JF, Hayes JD, Nishimoto SK. Plasmin-mediated proteolysis of osteocalcin. J Bone Miner Res. 1997; 12:1035–1042. [PubMed: 9200002]
43. Pandolfi A, Iacoviello L, Capani F, Vitacolonna E, Donati MB, Consoli A. Glucose and insulin independently reduce the fibrinolytic potential of human vascular smooth muscle cells in culture. Diabetologia. 1996; 39:1425–1431. [PubMed: 8960822]
44. Parfitt AM, Drezner MK, Glorieux FH, Kanis JA, Malluche H, Meunier PJ, Ott SM, Recker RR. Bone histomorphometry: standardization of nomenclature, symbols, and units. Report of the ASBMR Histomorphometry Nomenclature Committee. J Bone Miner Res. 1987; 2:595–610. [PubMed: 3455637]
45. Peters M, Schirmacher P, Goldschmitt J, Odenthal M, Peschel C, Fattori E, Ciliberto G, Dienes HP, Meyer zum Buschenfelde KH, Rose-John S. Extramedullary expansion of hematopoietic progenitor cells in interleukin (IL)-6-sIL-6R double transgenic mice. J Exp Med. 1997; 185:755–766. [PubMed: 9034153]
46. Phillips CL, Bradley DA, Schlotzhauer CL, Bergfeld M, Libreros-Minotta C, Gawenis LR, Morris JS, Clarke LL, Hillman LS. Oim mice exhibit altered femur and incisor mineral composition and decreased bone mineral density. Bone. 2000; 27:219–226. [PubMed: 10913914]
47. Poli V, Balena R, Fattori E, Markatos A, Yamamoto M, Tanaka H, Ciliberto G, Rodan GA, Costantini F. Interleukin-6 deficient mice are protected from bone loss caused by estrogen depletion. Embo J. 1994; 13:1189–1196. [PubMed: 8131749]
48. Ramirez F, Sakai LY, Dietz HC, Rifkin DB. Fibrillin microfibrils: multipurpose extracellular networks in organismal physiology. Physiol Genomics. 2004; 19:151–154. [PubMed: 15466717]
49. Renckens R, Roelofs JJ, de Waard V, Florquin S, Lijnen HR, Carmeliet P, van der Poll T. The role of plasminogen activator inhibitor type 1 in the inflammatory response to local tissue injury. J Thromb Haemost. 2005; 3:1018–1025. [PubMed: 15869599]
50. Roarck RJ. Formulas for Stress and Strain: McGraw-Hill. 2002
51. Roy ME, Nishimoto SK. Matrix Gla protein binding to hydroxyapatite is dependent on the ionic environment: calcium enhances binding affinity but phosphate and magnesium decrease affinity. Bone. 2002; 31:296–302. [PubMed: 12151082]
52. Rubin J, Rubin C, Jacobs CR. Molecular pathways mediating mechanical signaling in bone. Gene. 2006; 367:1–16. [PubMed: 16361069]
53. Schneiderman J, Sawdey MS, Keeton MR, Bordin GM, Bernstein EF, Dilley RB, Loskutoff DJ. Increased type 1 plasminogen activator inhibitor gene expression in atherosclerotic human arteries. Proc Natl Acad Sci U S A. 1992; 89:6998–7002. [PubMed: 1495992]
54. Shimomura I, Funahashi T, Takahashi M, Maeda K, Kotani K, Nakamura T, Yamashita S, Miura M, Fukuda Y, Takemura K, Tokunaga K, Matsuzawa Y. Enhanced expression of PAI-1 in visceral fat: possible contributor to vascular disease in obesity. Nat Med. 1996; 2:800–803. [PubMed: 8673927]

55. Stefansson S, Lawrence DA. The serpin PAI-1 inhibits cell migration by blocking integrin alpha V beta 3 binding to vitronectin. Nature. 1996; 383:441–443. [PubMed: 8837777]
56. Thogersen AM, Jansson JH, Boman K, Nilsson TK, Weinehall L, Huhtasaari F, Hallmans G. High plasminogen activator inhibitor and tissue plasminogen activator levels in plasma precede a first acute myocardial infarction in both men and women: evidence for the fibrinolytic system as an independent primary risk factor. Circulation. 1998; 98:2241–2247. [PubMed: 9826309]
57. Tumber A, Papaioannou S, Breckon J, Meikle MC, Reynolds JJ, Hill PA. The effects of serine proteinase inhibitors on bone resorption in vitro. J Endocrinol. 2003; 178:437–447. [PubMed: 12967336]
58. Turner CH, Takano Y, Hirano T. Reductions in bone strength after fluoride treatment are not reflected in tissue-level acoustic measurements. Bone. 1996; 19:603–607. [PubMed: 8968026]
59. Vassalli JD, Sappino AP, Belin D. The plasminogen activator/plasmin system. J Clin Invest. 1991; 88:1067–1072. [PubMed: 1833420]
60. Vaughan DE, Lazos SA, Tong K. Angiotensin II regulates the expression of plasminogen activator inhibitor-1 in cultured endothelial cells. A potential link between the renin-angiotensin system and thrombosis. J Clin Invest. 1995; 95:995–1001. [PubMed: 7884001]
61. Vial D, Monaghan-Benson E, McKeown-Longo PJ. Coordinate regulation of fibronectin matrix assembly by the plasminogen activator system and vitronectin in human osteosarcoma cells. Cancer Cell Int. 2006; 6:8. [PubMed: 16569238]
62. Wang X, Lee SR, Arai K, Tsuji K, Rebeck GW, Lo EH. Lipoprotein receptor-mediated induction of matrix metalloproteinase by tissue plasminogen activator. Nat Med. 2003; 9:1313–1317. [PubMed: 12960961]
63. Yang JN, Allan EH, Anderson GI, Martin TJ, Minkin C. Plasminogen activator system in osteoclasts. J Bone Miner Res. 1997; 12:761–768. [PubMed: 9144342]
64. Young MF. Bone matrix proteins: their function, regulation, and relationship to osteoporosis. Osteoporos Int. 2003; 14(Suppl 3):S35–S42. [PubMed: 12730768]

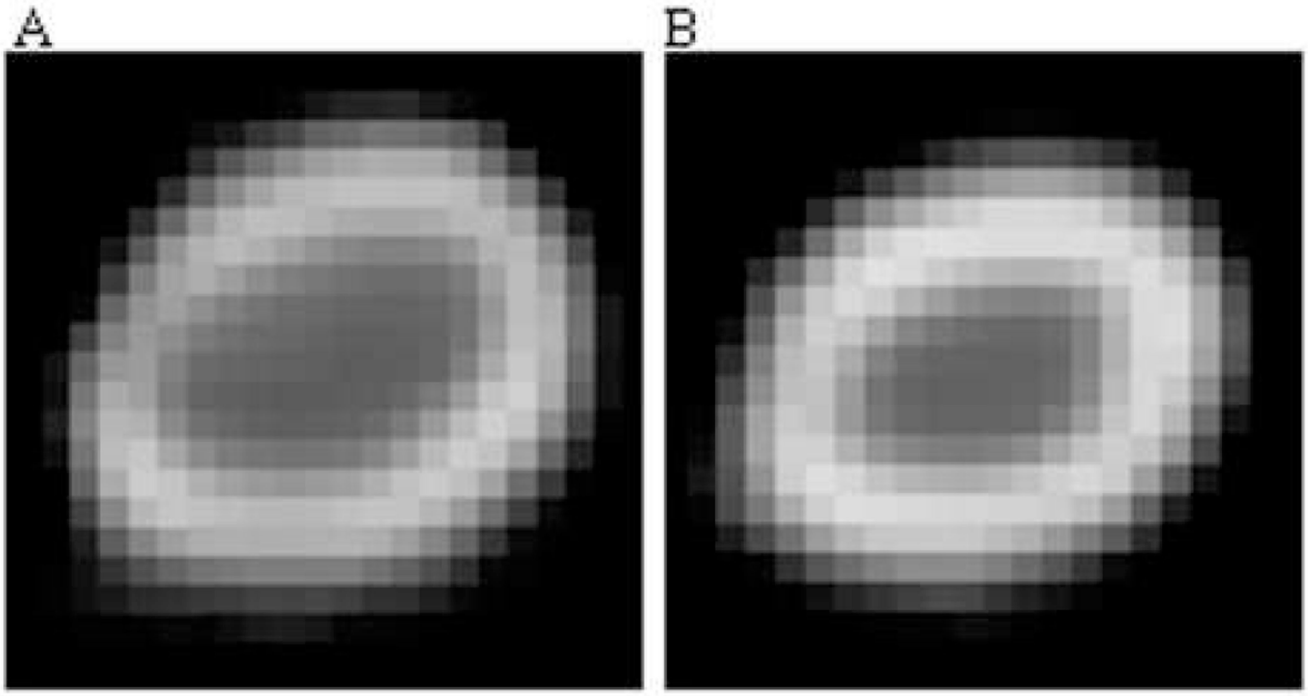

Figure I.

Thirty-two week female PAI-1.stab cortical bone had decreased major and minor periosteal/endosteal diameters as well as a lower polar moment of area compared to age-matched WT females. Representative femoral mid-slice μCT images from 32 week WT (A) and PAI-1.stab (B) female femora.

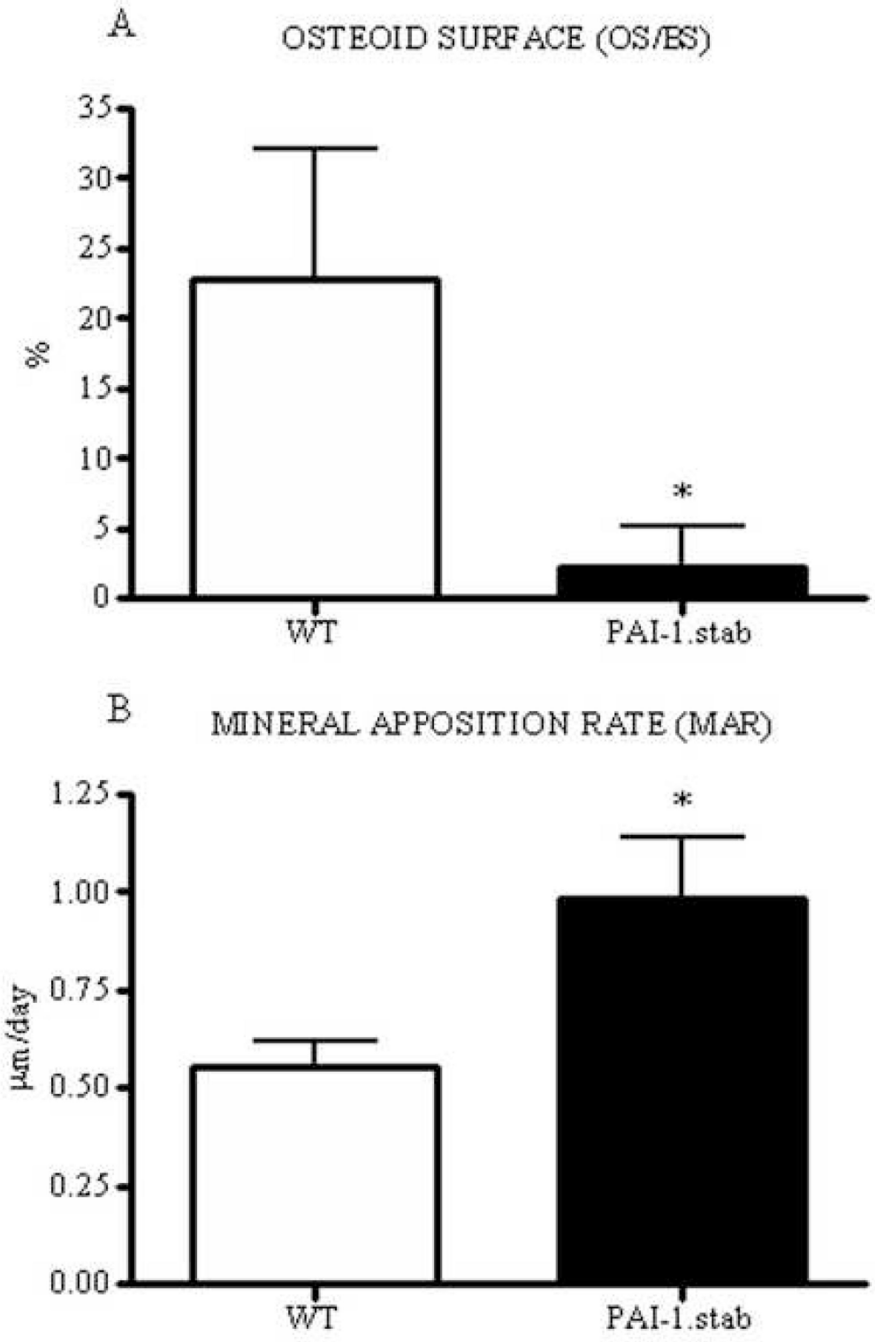

Figure II.

Twenty-eight week female PAI-1.stab *(shaded)* femora demonstrated reduced osteoid area, OS/BS (A), and increased mineral apposition rate, MAR (B) compared to age-matched WT females *(open)*. *Indicates significant difference relative to WT, $p<0.05$. (n=11)

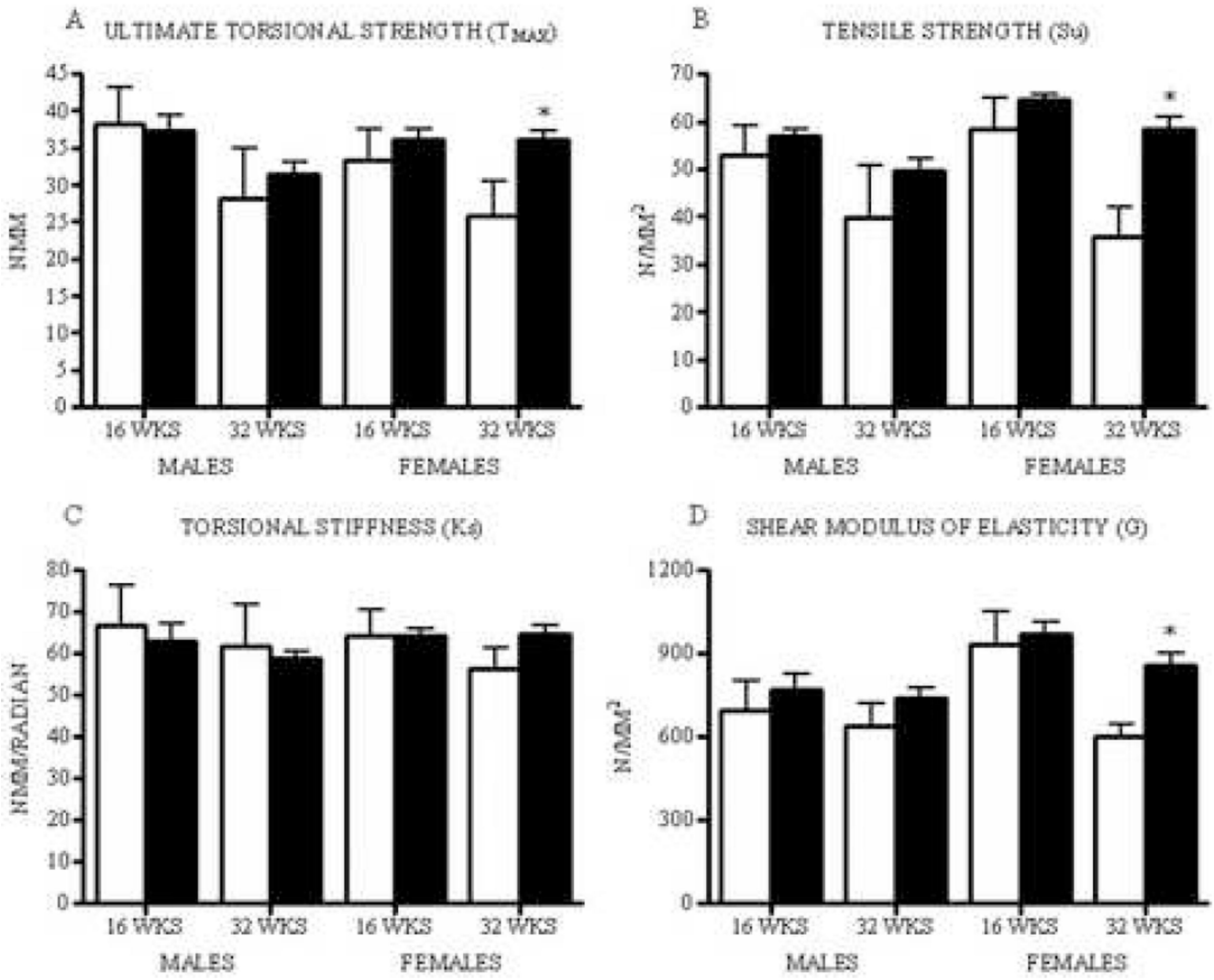

Figure III.

Thirty-two week female PAI-1.stab *(shaded)* femora demonstrated greater diaphyseal ultimate torsional strength, T_{max} (A), greater cortical bone tensile strength, Su (B), a trend towards greater torsional stiffness, Ks (C), and greater shear modulus of elasticity, G (D) compared to age-matched WT females *(open)*. *Indicates significant difference relative to age- and gender-matched WT, $p<0.05$. (n=7–9)

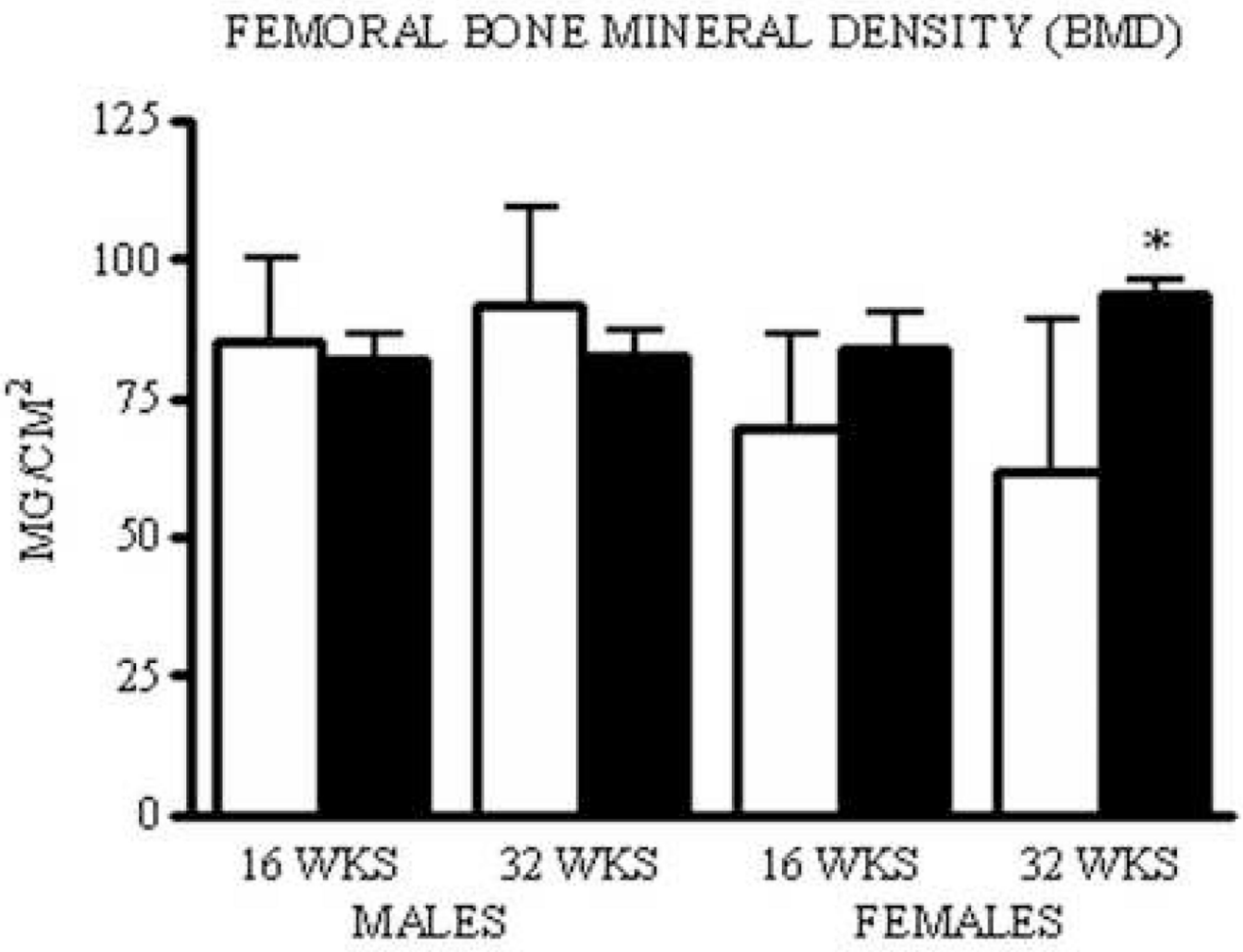

Figure IV.

Thirty-two week female PAI-1.stab *(shaded)* femora have greater bone mineral density compared to WT *(open)*. Indicates significant difference relative to age- and gender-matched WT, $p<0.05$. (n=10)

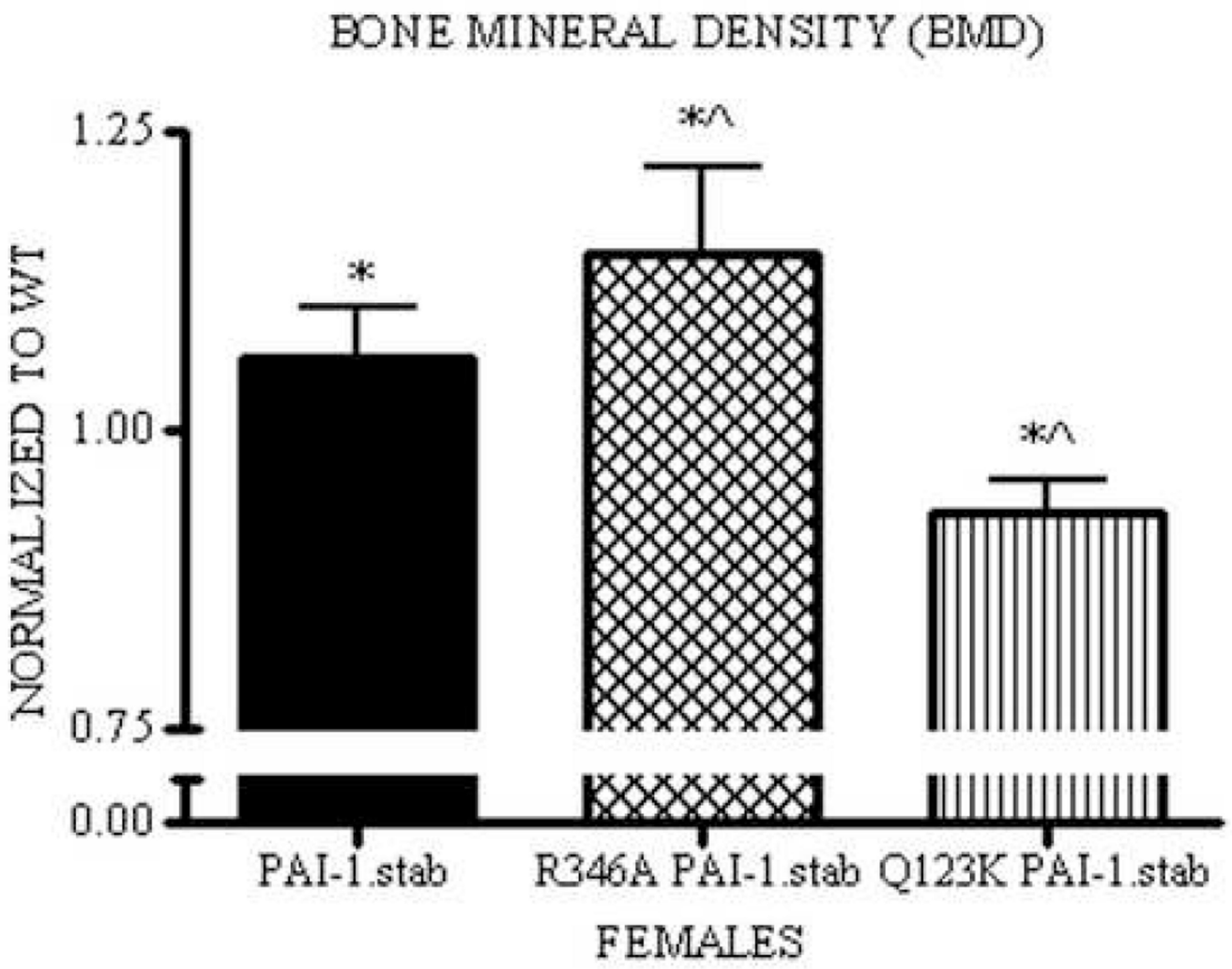

Figure V.

Thirty-two week PAI-1.stab females *(shaded)* have increased total skeletal BMD compared to WT. R346A PAI-1.stab females *(hatched)* have increased total skeletal BMD compared to WT and PAI-1.stab. Q123K PAI-1.stab females *(striped)* have decreased total skeletal BMD compared to PAI-1.stab and WT. BMD measures for each group are normalized to age-, gender-, and background-matched controls for comparison between strains. * Indicates significant difference relative to WT (1.00), ^ Indicates significant difference relative to PAI-1.stab,$p<0.05$. (n=6–10)

TABLE I

Geometric properties of femora from male and female PAI-1.stab and WT mice at 16 and 32 weeks of age (n=10), mean ± SD.

Parameters	Males				Females			
	16 weeks		32 weeks		16 weeks		32 weeks	
	WT	PAI-1. stab	WT	PAI-1. stab	WT	PAI-1. stab	WT	PAI-1. stab
Major Periosteal Diameter (mm)	2.00±0.09	1.86^{a}±0.13	2.00±0.06	1.86^{a}±0.06	1.78^{c}±0.05	1.72^{c}±0.07	1.90^{b}±0.05	1.78^{a}±0.11
Major Endosteal Diameter (mm)	1.04±0.07	0.94±0.11	1.06±0.07	0.91^{a}±0.07	0.88^{c}±0.07	0.81^{c}±0.05	1.03^{b}±0.08	0.82^{a}±0.07
Minor Periosteal Diameter (mm)	1.40±0.06	1.37±0.05	1.40±0.05	1.36±0.08	1.32^{c}±0.04	1.32±0.05	1.47^{b}±0.06	1.36^{a}±0.03
Minor Endosteal Diameter (mm)	0.56±0.07	0.54±0.07	0.52±0.08	0.55±0.08	0.51±0.02	0.49±0.04	0.63^{bc}±0.05	0.52^{a}±0.06
Cortical Bone Width (mm)	0.45±0.03	0.44±0.02	0.45±0.03	0.44±0.02	0.42±0.03	0.43±0.03	0.43±0.01	0.45±0.04
Cortical Area (mm^2)	1.66±0.12	1.56±0.15	1.70±0.15	1.47^{a}±0.09	1.44^{c}±0.10	1.40±0.15	1.56±0.09	1.48±0.14
Polar Moment of Area (mm^4)	0.67±0.11	0.58±0.10	0.66±0.08	0.56±0.09	0.48^{c}±0.05	0.47±0.07	0.68^{b}±0.08	0.53^{a}±0.07
Femur Length (mm)	15.51±0.59	15.38±0.52	15.71±0.35	15.40±0.42	14.74^{c}±0.60	15.12±0.54	16.06^{b}±0.47	15.77±0.47

^{a}Indicates significant genotype-dependent difference; WT vs PAI-1 for same gender and age; $p<0.05$

^{b}Indicates significant age-dependent difference; 16 weeks vs 32 weeks for same gender and genotype; $p<0.05$

^{c}Indicates significant gender-dependent difference; male vs female for same age and genotype; $p<0.05$

TABLE II

Histomorphometric properties of trabecular bone from female PAI-1.stab and WT mice at 28 weeks of age (n=11); mean +SD.

Parameters	WT	PAI-1.stab
Trabecular Bone Volume (BV/TV)(%)	4.37±1.26	4.35 ± 1.83
Trabecular Number (Tr.N.)(mm^{-1})	1.35±0.32	1.31 ± 0.53
Trabecular Thickness (Tr.Th.)(μm)	32.01 ±4.89	33.24 ± 6.44
Trabecular Spacing (Tr.Sp.)(μm)	753.6 ± 228.7	881.5 ± 459.5
Osteoid Surface (OS/BS)(%)	22.85 ± 9.17	2.23 ± 2.88[a]
Mineral Apposition Rate (MAR)(μm/day)	0.55 ± 0.07	0.98 ± 0.15[a]

[a] Indicates significant difference between WT and PAI-1.stab; $p<0.05$

TABLE III

Biomechanical properties of femora from male and female PAI-1.stab and WT mice at 16 and 32 weeks of age (n=7–9), mean ± SD.

Parameters	Males				Females			
	16 weeks		32 weeks		16 weeks		32 weeks	
	WT	PAI-1. stab	WT	PAI-1. stab	WT	PAI-1. stab	WT	PAI-1. stab
Ultimate Torsional Strength (Nmm)	38.20±4.94	37.38±6.35	28.24^{b}±6.79	31.44±5.12	33.36±4.14	36.16±3.54	25.84±4.72	36.00^{a}±3.56
Torsional Stiffness (Nmm/radian)	66.82±9.35	63.09±11.66	61.88±9.97	58.80±5.11	64.38±5.98	64.17±4.72	56.12±5.15	64.69±5.80
Bone Tensile Strength (N/mm^2)	52.96±6.11	56.76±5.27	39.89b±10.71	49.56±8.40	58.50±6.48	64.52^{c}±3.44	35.92^{b}±6.01	58.28^{a}±7.51
Shear Modulus of Elasticity (N/mm^2)	692.4±106.5	766.2±179.2	640.6±76.5	738.9±108.9	933.4^{c}±119.7	968.4^{c}±110.2	599.0^{b}±47.9	858.4^{a}±123.2
Strain Energy to Failure (Nmm)	15.35±8.28	21.05±11.33	12.99±9.75	12.29±7.60	12.10±5.02	14.49±1.32	9.78±5.02	11.36±3.27

^{a}Indicates significant genotype-dependent difference; WT vs PAI-1 for same gender and age; $p<0.05$

^{b}Indicates significant age-dependent difference; 16 weeks vs 32 weeks for same gender and genotype; $p<0.05$

^{c}Indicates significant gender-dependent difference; male vs female for same age and genotype; $p<0.05$

TABLE IV

Mineral composition of femora from male and female PAI-1.stab and *WT* mice at 16 and 32 weeks of age (n=8–11), mean + SD.

Parameters	Males				Females			
	16 weeks		32 weeks		16 weeks		32 weeks	
	WT	PAI-1. stab	WT	PAI-1. stab	WT	PAI-1. stab	WT	PAI-1. stab
F (ppm)	673.3±38.4	350.9^{a}±31.3	1119.0^{b}±95.7	630.3^{ab}±54.0	629.6±48.0	332.0^{a}±58.7	1422.0^{bc}±61.9	513.0^{abc}±48.9
Mg (ppm)	5239±156	5056±191	4653±207	4613±183	5672±763	4662^{a}±274	4939±717	4927±1353
K (ppm)	158.6±63.0	233.8±114.0	152.0±62.2	185.1±63.4	122.9±50.6	262.2^{a}±160.6	160.9±63.2	202.7±58.4
Cl (ppm)	74.53±24.42	93.84±50.15	72.70±24.33	136.50^{a}±26.78	76.97±26.03	78.97±40.70	54.62±21.56	71.68^{c}±28.17
Zn (ppm)	226.3±58.7	177.3±39.1	224.1±50.4	154.9±39.3	227.8±72.6	213.1±59.1	285.4±83.7	259.7^{c}±76.9
Na (ppm)	4080±190	4093±204	4287±133	4651±165	4399±637	4199±246	3997±613	4691±1555
Ca (ppm)	251328±3380	244329±7742	247766±5223	258828±3629	264032±35345	236207±12023	232935±33744	257048±75666
P (ppm)	117328±1358	115085±3345	116700±2410	120008±2582	127384±16864	114662±5031	117673±2589	129449±30217
Ca/P	2.14±0.03	2.12±0.04	2.12±0.04	2.16±0.03	2.07^{c}±0.03	2.06^{c}±0.03	2.06^{c}±0.04	2.10±0.06

^{a}Indicates significant genotype-dependent difference; WT vs PAI-1 for same gender and age; $p<0.05$

^{b}Indicates significant age-dependent difference; 16 weeks vs 32 weeks for same gender and genotype; $p<0.05$

^{c}Indicates significant gender-dependent difference; male vs female for same age and genotype; $p<0.05$